Published in final edited form as:
J Biomed Nanotechnol. 2008 December 1; 4(4): 482–490. doi:10.1166/jbn.2008.014.

Synthesis and Characterization of Thermo-Sensitive Nanoparticles for Drug Delivery Applications

Maham Rahimi[1,2], **Sunitha Kilaru**[1,2], **Ghida El Hajj Sleiman**[1,2], **Anas Saleh**[3], **Dmitry Rudkevich**[3,†], and **Kytai Nguyen**[1,2]

[1]Biomedical Engineering Program, University of Texas Southwestern Medical Center at Dallas and University of Texas at Arlington

[2]Department of Bioengineering, University of Texas at Arlington

[3]Department of Chemistry, University of Texas at Arlington

Abstract

The aim of this research project was to develop new temperature sensitive nanoparticles that have a lower critical solution temperature (LCST) that is above body temperature and can be incorporated with various molecules at the surface. The poly(*N*-isopropylacrylamide-co-acrylamide-co-allylamine) (NIPA-AAm-AH) nanoparticles were synthesized through a free radical polymerization method. NIPA was polymerized with AAm and AH to increase the LCST and to provide amine groups for functionalization, respectively. Using transmission electron microscopy (TEM) and laser scattering technology, the sizes of these nanoparticles were found to be inversely proportional to the surfactant concentrations. In addition, the LCST of the 100-nm NIPA-AAm-AH nanoparticles was approximately 40 °C measured by a spectrophotometer. The chemical composition of the NIPA-AAm-AH nanoparticles determined with Fourier transform infrared spectroscopy (FTIR) and nuclear magnetic resonance (NMR) also confirmed the presence of functional groups of each monomer. The nanoparticles were also successfully conjugated to bovine anti-rabbit IgG-Texas Red as a model for future bioconjugation. Furthermore, nanoparticles did not show significant cytotoxicity activity against human fibroblast cells. Finally, doxorubicin (DOX) was used in order to investigate the drug release profiles of the NIPA-AAm-AH nanoparticles at different temperatures. The results indicated that DOX was released more at 41 °C compared to that of 37 °C and 4 °C, which is evidence for temperature sensitivity of the nanoparticles. Future work will investigate the pharmacological and targeted capabilities of the synthesized nanoparticles conjugated to antibodies for possible application in controlled and targeted drug delivery.

1. INTRODUCTION

Temperature sensitive polymers have been attracting much attention because of their applications in various fields, especially in biotechnology and medicine. These applications include cell culture, tissue engineering, wound healing, and drug delivery systems.[1–6] For instance, temperature sensitive nanoparticles have been developed as controlled release drug delivery carriers used in cancer treatment and gene therapy.[2, 7] A major advantage of the temperature sensitive nanoparticles as a drug delivery system is their phase change due to temperature. Temperature sensitive polymers undergo a reversible phase transition at a lower

Correspondence to: Kytai Nguyen.

†Deceased.

critical solution temperature (LCST), where the hydrogel hydrophobically collapses and squeezes water out in an entropically favored fashion. A reversible swelling and shrinking behavior based on this phenomenon has been used as a means to control loading and releasing of various therapeutic agents. For example, drugs can be loaded in these nanoparticles at temperatures below the LCST. These nanoparticles are then delivered to the specific locations and collapsed to release the drugs when the temperature at these regions is raised above the LCST. These drug release responses to changes in temperature make temperature-sensitive nanoparticles attractive for controlled release drug delivery applications.

A variety of polymers have been used to produce the temperature sensitive nanoparticles as drug delivery systems. Both natural polymers such as chitosan, peptide, and cellulose as well as synthetic polymers like poly *N*-isopropylacrylamide (NIPA), poly(*N*-isopropylacrylamide-co-acrylamide) (NIPA-AAm), poloxamers, and poly(lactic acid-co-ethylene glycol) have been employed.[8–14] Of these polymers, NIPA and its copolymers have been studied extensively.[15, 16] NIPA is capable of undergoing reversible swelling and shrinking events at a LCST of 34 °C. Block copolymers containing NIPA and AAm interpenetrating networks have been used to formulate nanoparticles that have a LCST above body temperature.[17] Although the copolymer of NIPA and AAm is useful to develop controlled drug delivery systems, it is difficult to incorporate other molecules such as antibodies and proteins onto NIPA-AAm nanoparticles to increase their targeted capabilities. With these nanoparticles, conjugation is possible by performing additional synthetic steps which would introduce impurities altering the LCST significantly. Consequently, there is a need to introduce another monomer to the copolymer of NIPA and AAm to functionalize the nanoparticles without changing its LCST dramatically.

Previously we have reported the synthesis of NIPA nanoparticles that has LCST of 34 °C.[21] The objective of this research project was to develop novel temperature-sensitive nanoparticles that consist of both a LCST above body temperature for controlled drug delivery in response to changes in temperature and functional groups for conjugation. These nanoparticles could be used in targeted and controlled drug delivery applications. We applied an alternative approach to functionalize NIPA-AAm nanoparticles with allylamine. Polymerization of NIPA with allylamine has shown to not significantly alter LCST of the NIPA polymer.[18] In addition, allylamine has amine groups for conjugation of bioactive molecules including antibodies and specific ligands.[18] The novel NIPA-AAm-AH nanoparticles were synthesized by a free radical polymerization. The size and size distribution of the nanoparticles were analyzed utilizing a laser scattering particle sizer (Nanotrac.) and transmission electron microscopy (TEM). In addition, the chemical composition of these nanoparticles was investigated using Fourier transform infrared spectroscopy (FTIR), proton nuclear magnetic resonance (^{1}H NMR), and carbon-13 nuclear magnetic resonance (^{13}C NMR).In order to assess the conjugation capability of the synthesized nanoparticles, fluorescent antibodies were further incorporated to the NIPA-AAm-AH nanoparticles, and its fluorescence was imaged via an enhanced optical microscope (Cytoviva) to assess the success of this conjugation. Furthermore, MTS assays and 3T3 fibroblast cells were used in order to investigate the cytotoxicity of the NIPA-AAm-AH nanoparticles. The amount of drugs (e.g., doxorubicin, DOX) released from the nanoparticles at temperatures below and at its LCST was also analyzed using a fluorometer.

2. MATERIALS

All chemicals such as monomers, *N*-isopropylacrylamide (NIPA), acrylamide (AAm), allylamine hydrochloric acid (AH), initiators, ammonium persulfate (APS), surfactant, sodium dodecyl sulfate (SDS), activator, *N*,*N*,*N*′,*N*′-tetramethyl ethylene diamine (TEMED), and cross-linking agent, *N*,*N*′-methylenebisacrylamide (BIS), *N*-(3-dimethylaminopropyl)-*N*′-ethylcarbodiimide hydrochloride (EDC), 2-(*N*-Morpholino)ethanesulfonic acid sodium salt

(MES) buffer solution, and doxorubicin hydrochloride were purchased from Sigma-Aldrich, unless otherwise specified. Bovine anti-rabbit IgG-Texas Red (IgG-TR) was purchased from Santa Cruz. Cell media, serum, and supplements were obtained from Invitrogen.

3. METHODS

3.1. Synthesis of Poly(NIPA-co-AAm-co-AH) Nanoparticles

The polymerization of poly(*N*-isopropylacrylamide-co-acrylamide-co-allylamine) was carried out in de-ionized water at room temperature using BIS as the cross-linking agent, SDS as the surfactant, and APS and TEMED as a pair of redox initiators as previously described.[19] To make (NIPA-AAm-AH) nanoparticles, 1.108 g of NIPA, 0.143 g of AAm, 378 μL of AH, and 0.0262 g of BIS were dissolved in 100 ml of de-ionized water. SDS was added to the solution at various concentrations (1.53, 0.298, 0.198, and 0.0243 mM) under continuous stirring. The solution was purged with argon for 30 minutes. Then, 0.078 g of APS and 101 μL of TEMED were added to the solution and the reaction was carried out at room temperature under Argon for 2 hours. After the reaction was completed, the nanoparticles were dialyzed against de-ionized water using 10 kDa molecular weight cut off for 3 days to remove surfactants and un-reacted materials.

3.2. Particle Size and Particle Size Distribution

Measurement of the average diameter of nanoparticles was performed in de-ionized water by the dynamic light scattering technology (Nanotrac. 150, Microtrac. Inc.). The size measurement was performed at room temperature (25 °C).

3.3. Transmission Electron Microscopy (TEM)

TEM (JEOL 1200 EX) was used to determine the size and shape of the synthesized nanoparticles. In general, samples were prepared by drop casting an aqueous dispersion of nanoparticles onto a carbon coated copper grid. The grid was then dried at room temperature before viewing under the microscope. The nanoparticles were stained with phosphotungstic acid (PTA) at a concentration of 0.01 wt% before observation.

3.4. Fourier Transform Infrared Spectroscopy (FTIR)

Dried samples were dissolved in dichloromethane and a drop of this solution was placed on NaCl discs. FTIR spectra were recorded in the transmission mode using a Thermo FT-IR Nicolet-6700. The spectrum was taken from 4000 to 400 cm^{-1}.

3.5. ^{1}H NMR and ^{13}C NMR Studies

^{1}H NMR and ^{13}C NMR spectra were recorded at 25 °C on JEOL 300 and 500 MHz spectrometers, respectively. Chemical shifts were measured relative to residual non-deuterated solvent resonances. The spectrum of the NIPA-AAm-AH was recorded in deuterated dimethyl sulfoxide (DMSO) solution.

3.6. LCST Determination

Optical transmittance of the aqueous nanoparticle solution (2 mg/ml) at various temperatures (25–45 °C with 1 °C intervals) was measured at 650 nm with a UV-Vis spectrophotometer (Cary 50 UV-Vis spectrophotometer coupled with PCB-150 circulating water bath).

3.7. Conjugation

In order to test the conjugation capability of the NIPA-AAm-AH nanoparticles, red IgG-TR (bovine anti-rabbit IgG-Texas Red) was used. These fluorescent antibodies were conjugated

onto the nanoparticle surfaces via carbodiimide chemistry. In brief, 0.01 g of NIPA-AAm-AH nanoparticles were dissolved in 0.5 ml of MES (0.1 M) buffer solution containing 0.01 g of EDC. The reaction was mixed well for 10 minutes at room temperature.0.2 mg of IgG-TR was added to the above solution and allowed to react with nanoparticles for 2 hours at room temperature under stirring and dark conditions. The nanoparticle solution was dialyzed under dark conditions (MWCO 100 kDa) against DI-H_2O for 1 week to remove unreacted IgG-TR. The sample was lyophilized and resuspended in 50% glycerol in water before imaging by an enhanced optical fluorescent microscope (Cytoviva).

3.8. Cytotoxicity Studies

Cytotoxicity studies were carried out on human 3T3 fibroblast cells (NIH) using (3-(4,5-dimethylthiazol-2-yl)-5-(3-carboxymethoxyphenyl) -2-(4-sulfophenyl) - 2H-tetrazolium (MTS) assays (following manufacturer (Promega)'s instructions).[20] This assay is based on the competence of the live cells to reduce the MTS into formazan. In order to investigate the biocompatibility of our nanoparticles, the cell viability of 3T3 fibroblast cells was studied. The cells were incubated with synthesized nanoparticles at various concentrations (16, 31, 62, 125, 250, and 500 μg/ml). The cell viability was determined after 24 and 48 hours incubation. The cytotoxicity results were presented as the percentage of viable cells in each sample in comparison to controls (cells not treated with the nanoparticles).

3.9. Drug Loading

For drug loading and release studies, a cancer drug, doxorubicin (DOX), was used. In brief, 10 mg of lyophilized nanoparticles and 5 mg of DOX were dispersed in phosphate buffer solution (PBS). The solution was stirred at 4 °C for 3 days to allow DOX to entrap within the nanoparticle network. The nanoparticle solution was dialyzed against PBS for 3 hours (this time was predetermined for optimal separation of the unencapsulated drug) to remove the free DOX. The dialysate was then analyzed using an Infinite M200 plate reader (Tecan) in order to determine the amount of DOX in the dialysate (λ_{ex} 470 nm and λ_{em} 585 nm). This value was then compared with the total amount of DOX to determine the DOX loading efficiency of the nanoparticles. Loading efficiency was calculated according to the following formula:

$$\% \quad \text{Loading Efficiency} = \frac{\text{total} \quad [\text{DOX}] \quad \text{used} - [\text{DOX}] \quad \text{present in dialysate}}{\text{total} \quad [\text{DOX}] \quad \text{used}} \times 100\%$$

3.10. *In Vitro* Drug Release Kinetics

In order to study the drug release profile of the synthesized nanoparticles, 2 ml of the drug loaded nanoparticle solution was placed inside dialysis bags with a molecular weight cutoff (MWCO) of 10,000 Da. Samples were dialyzed against PBS at 4 °C, 37 °C, and 41 °C. At designated time intervals, 1 ml of dialysate was removed from each sample and stored at −20 °C for later analysis. The dialysate volume was reconstituted by adding 1 ml of fresh PBS to each sample. After experiments, the dialysate samples were analyzed using an Infinite M200 plate reader (λ_{ex} 470 nm and λ_{em} 585 nm) to quantify the amount of DOX released.

4. RESULTS AND DISCUSSION

In this work we intended to synthesize temperature sensitive nanoparticles with a copolymer of NIPA (NIPA-AAm-AH), which have both the LCST above body temperature and the amine functional groups for incorporation of biomolecules.Free radical polymerization was used to synthesize NIPA-AAm-AH nanoparticles. Several techniques such as particle sizer, TEM, FTIR, NMR, enhanced optical microscopy (Cytoviva), and UV-Vis spectrophotometer were used to characterize the synthesized nanoparticles. In addition, the cytotoxicity of the

nanoparticles on 3T3 fibroblast cells was evaluated using MTS assays. Finally, the drug release behavior from these nanoparticle was analyzed using DOX as a model drug. The results from each characterization method are discussed below.

4.1. Particle Size, Size Distribution, and Morphology

The average size of the synthesized NIPA-AAm-AH nanoparticles was analyzed using dynamic light scattering technology. Different concentrations of surfactant (SDS) were used to synthesize nanoparticles with various sizes. The size of the nanoparticles increases as the concentration of SDS decreases, as shown in Figure 1. It is evident that the size of the nanoparticles is inversely proportional to the concentration of SDS. This type of relationship between surfactants and the nanoparticle size is consistent with previous observations.[21] However, the relationship was found to be nonlinear at SDS concentrations higher than 0.298 mM. Since we selected 100-nm nanoparticles for later studies, several characterization techniques were performed for this particular size only. The nanoparticle size distribution of 100 nm particles is shown in Figure 2. The size of NIPA-AAm-AH nanoparticles was also analyzed using TEM. The black background around the nanoparticles is the phosphotungstic acid stain that was used to define the outer edge of the nanoparticles (Fig. 3). TEM revealed that the preparation procedure gave spherical nanoparticles. The size noted by TEM was within the range of size measured by Nanotrac.

4.2. Particle Composition

The chemical composition of the synthesized nanoparticle was analyzed using both FTIR and NMR. As shown in Figure 4(a) for FTIR, the stretching vibration appearing in the range of 2900–3100 cm^{-1} corresponds to C–H bands. The IR peak at 3423.6 cm^{-1} corresponds to the stretching vibration of the primary amine group in the NIPA-AAm-AH. The peak from the secondary amine group of NIPA is observed around 3308.7 cm^{-1}. Furthermore, the carbonyl group of NIPA and AAm is observed at 1655 cm^{-1}. These peaks indicate that the NIPA-AAm-AH consists of functional groups corresponding to their constitute monomers as shown in Figure 4(b).

In order to analyze the chemical composition of the NIPA-AAm-AH in more detail, proton (^{1}H NMR) and carbon nuclear magnetic resonance (^{13}C NMR) were used. In ^{1}H NMR (Fig. 5(a)), we observed the backbone hydrogen of the NIPA-AAm-AH at 1.89 (c, broad, 1 H) and 1.46 (b, broad, 2 H). The hydrogen attached to the isopropyl of NIPA was observed at 3.78 (d, multiplet, 1 H), and the hydrogen of methyl groups in NIPA was observed at 1.02 (a, multiplet, 6 H). The broad peak at 7.40 to 7.80 ppm is from the hydrogen in the amide groups. The ^{13}C NMR (Fig. 5(b)) identified the carbonyl group of AAm at 177.98 ppm and the carbonyl group of NIPA at 173.96 ppm. Furthermore, the composition of the NIPA-AAm-AH was determined by using ^{13}C NMR and titration. As shown in Table I, the composition of the NIPA-AAm-AH was approximately close to those in the feed (or original amounts of materials), implying that polymerization was as expected.

4.3. LCST Determination

To determine the temperature at which the phase transition occurs in the nanoparticles, UV-Vis spectrophotometer was used. As shown in Figure 6, the LCST of NIPA nanoparticles was 34 °C. The rate at which the transition occurs slowly changes around 32 °C, and then the intensity sharply decreases at 34 °C. Also shown in Figure 6, the phase transition of NIPA-AAm and NIPA-AAm-AH nanoparticles occurs sharply at 39 °C and 40 °C, respectively. In addition to the LCST measurements, the phase transition of the nanoparticles can easily be seen when the solution goes from clear to cloudy at each specific LCST, as shown in Figure 7.

4.4. Conjugation

In order to assess the capability of our nanoparticles for future bioconjugation, IgG-TR was utilized to conjugate onto the nanoparticles. IgG-TR was conjugated to nanoparticles using the carbodiimide chemistry, as shown in Figure 8(a). Enhanced optical fluorescence microscopy was used to assess the attachment of IgG-TR onto nanoparticles. As Figure 8(b) indicates, a bright red color was observed in our NIPA-AAm-AH nanoparticles, whereas this fluorescence was not seen in NIPA-AAm nanoparticles (control). These results indicate that our NIPA-AAm-AH nanoparticles have amine functional groups available which can be utilized for conjugation of other molecules.

4.5. Cytotoxicity Studies

The cell viability was determined using MTS assays at different time points. As shown in Figure 9, there is no significant difference in the cell viability between control cells and cells exposed to nanoparticles, especially at concentrations less than 250 μg/ml. For all concentrations, the values of the cell toxicity are less than 15% at both time points. These results indicate that the synthesized nanoparticles exhibit low cytotoxicity, satisfying one of the major criteria required for a new drug delivery system.

4.6. Drug Loading Efficiency and Release Kinetics

Using DOX as a model cancer drug, we found that approximately 66% of the incubated DOX was loaded into the NIPA-AAm-AH nanoparticles. In addition, the cumulative percent release of DOX at 41 °C was significantly higher than at 37 °C and 4 °C (Fig. 10). This indicates that the NIPA-AAm-AH nanoparticles are temperature sensitive polymers whereby the nanoparticles collapse upon themselves and squeeze the drug out at its LCST. After 72 hours, 84% of the encapsulated DOX was released at 41 °C, whereas at 37 °C and 4 °C approximately 31% and 38%, respectively, were released. The release profile of the DOX over the first 30 minutes is also shown in Figure 10. After 30 minutes, the cumulative percent release of DOX is only 0.045% and 0.27% at 4 °C and 37 °C, respectively, whereas at 41 °C it is 2.5%.

5. CONCLUSION

In this study novel temperature-sensitive nanoparticles were developed from NIPA-AAm-AH. These nanoparticles have both a LCST above body temperature (40 °C) and amine functional groups. These nanoparticles can be used for controlled drug delivery due to their temperature sensitive properties. Due to their amine functional groups, these nanoparticles can also be attached to various biomolecules for targeted drug delivery. Our results indicated that as the surfactant concentration increased, the size of the nanoparticles decreased. The chemical composition analysis has shown that the nanoparticles consist of three components with their functional group clearly visible in FTIR and NMR. The amine groups of the nanoparticles were successfully conjugated to IgG-TR as a model for future bioconjugation. These nanoparticles also demonstrated biocompatibility property as shown by the cytotoxicity study on fibroblast cells. Furthermore, the drug release studies indicated that drugs released from these nanoparticles were in response to changes in temperature with the highest percentage of release occurring at the LCST of NIPA-AAm-AH nanoparticles. In the future, we will investigate the targeting capability of the synthesized nanoparticles and the pharmacological effects of drug-loaded and antibody conjugated NIPA-AAm-AH nanoparticles for drug delivery applications.

Acknowledgments

The FTIR spectrum was obtained from the UTA Characterization Center for Materials and Biology. The TEM work was performed at the University of Texas Southwestern Medical Center Molecular and Cellular Imaging Facility. We

would like to acknowledge the financial support from the American Heart Association Scientist Development Award 073520N and NIH grants HL082644 and HL091232 (Kytai Nguyen).

References and Notes

1. Chen H, Gu Y, Hub Y, Qian Z. Characterization of pH-and temperature-sensitive hydrogel nanoparticles for controlled drug release. PDA J. Pharm. Sci. Technol 2007;61:303. [PubMed: 17933211]
2. Ozdemir N, Tuncel A, Kang M, Denkbas EB. Preparation and characterization of thermosensitive submicron particles for gene delivery. J. Nanosci. Nanotechnol 2006;6:2804. [PubMed: 17048486]
3. Yan H, Tsujii K. Potential application of poly(*N*-isopropylacrylamide) gel containing polymeric micelles to drug delivery systems. Colloids Surf. B. Biointerfaces 2005;46:142. [PubMed: 16300934]
4. Shimizu T, Yamato M, Isoi Y, Akutsu T, Setomaru T, Abe K, Kikuchi A, Umezu M, Okano T. Fabrication of pulsatile cardiac tissue grafts using a novel 3-dimensional cell sheet manipulation technique and temperature-responsive cell culture surfaces. Circ. Res 2002;90:e40. [PubMed: 11861428]
5. Vernon B, Gutowska A, Kim SW, Bae YH. Thermally reversible polymer gels for biohybrid artificial pancreas. Macromol. Symp 1996;109:155.
6. Sarkhosh K, Tredget EE, Uludag H, Kilani RT, Karami A, Li Y, Iwashina T, Ghahary AJ. Temperature-sensitive polymer-conjugated IFN-γ induces the expression of IDO mRNA and activity by fibroblasts populated in collagen gel (FPCG). Cell. Physiol 2004;201:146.
7. Needham D, Dewhirst MW. The development and testing of a new temperature-sensitive drug delivery system for the treatment of solid tumors. Adv. DrugDeliv. Rev 2001;53:285.
8. Ruel-Gariâepy E, Shive M, Bichara A, Berrada M, Le Garrec D, Chenite A, Leroux JC. A thermosensitive chitosan-based hydrogel for the local delivery of paclitaxel. Eur. J. Pharm. Biopharm 2004;57:53. [PubMed: 14729080]
9. Pochan DJ, Schneider JP, Kretsinger J, Ozbas B, Rajagopal K, Haines L. Thermally reversible hydrogels via intramolecular folding and consequent self-assembly of a de novo designed peptide. J. Am. Chem. Soc 2003;125:11802. [PubMed: 14505386]
10. Tate MC, Shear DA, Hoffman SW, Stein DG, Laplaca MC. Biocompatibility of methylcellulose-based constructs designed for intracerebral gelation following experimental traumatic brain injury. Biomaterials 2001;22:1113. [PubMed: 11352091]
11. Schild HG. Poly(*N*-isopropylacrylamide): Experiment, theory and application. Prog. Polym. Sci 1992;17:163.
12. Han CK, Bae YH. Inverse thermally-reversible gelation of aqueous N -isopropylacrylamide copolymer solutions. Polymer 1998;39:2809.
13. Cabana A, Ait-Kadi A, Juhasz J. Study of the gelation process of polyethylene oxidea-polypropylene oxideb-polyethylene oxideacopolymer (Poloxamer 407) aqueous solutions. J. Colloid Interface Sci 1997;190:307. [PubMed: 9241171]
14. Jeonga B, Baeb YH, Kim SW. Drug release from biodegradable injectable thermosensitive hydrogel of PEG-PLGA-PEG tri-block copolymers. J. Control. Release 2000;63:155. [PubMed: 10640589]
15. Zintchenko A, Ogris M, Wagner E. Temperature dependent gene expression induced by PNIPAM-based copolymers: Potential of hyperthermia in gene transfer. Bioconjugate Chem 2006;17:766.
16. Chilkoti A, Drehera MR, Meyera DE, Raucher D. Targeted drug delivery by thermally responsive polymers. Polym. Conjug. Cancer Ther 2002;54:613.
17. Meyera DE, Shina BC, Konga GA, Dewhirstb MW, Chilkoti A. Drug targeting using thermally responsive polymers and local hyperthermia. J. Control. Release 2001;74:213. [PubMed: 11489497]
18. Hu Z, Huang G. A new route to crystalline hydrogels, guided by a phase diagram. Angew. Chem. Int. Ed. Engl 2003;42:4799. [PubMed: 14562353]
19. Yallapu MM, Vasir JK, Jain TK, Vijayaraghavalu S, Labhasetwar V. Synthesis, characterization and antiproliferative activity of rapamycin-loaded poly(*N*-isopropylacrylamide)-based nanogels in vascular smooth muscle cells. J. Biomed. Nanotechnol 2008;4:16.

20. Malich G, Markovic B, Winder C. The sensitivity and specificity of the MTS tetrazolium assay for detecting the in vitro cytotoxicity of 20 chemicals using human cell lines. Toxicology 1997;124:179. [PubMed: 9482120]

21. Ramanan RM, Chellamuthu P, Tang L, Nguyen KT. Development of a temperature-sensitive composite hydrogel for drug delivery applications. Biotechnol. Prog 2006;22:118. [PubMed: 16454501]

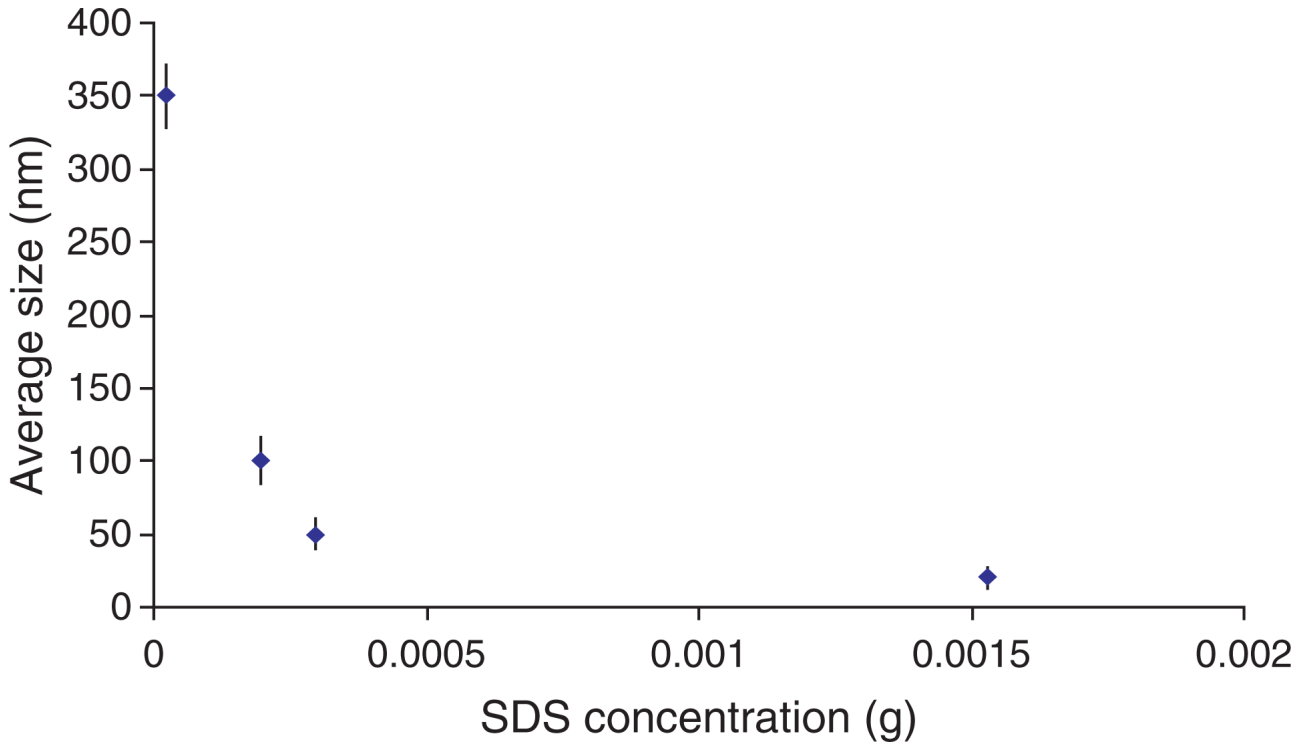

Fig. 1.
Effect of SDS concentrations on the mean size of nanoparticles (the result is represented as mean ± S.D., $n = 3$).

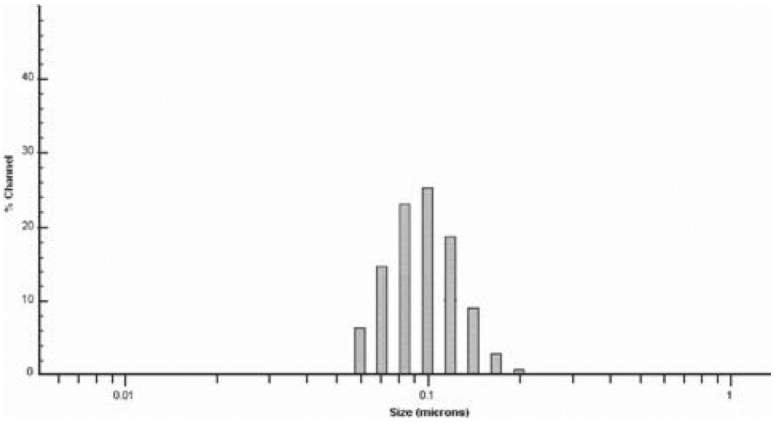

Fig. 2.
Particle size distribution of 100-nm nanoparticles.

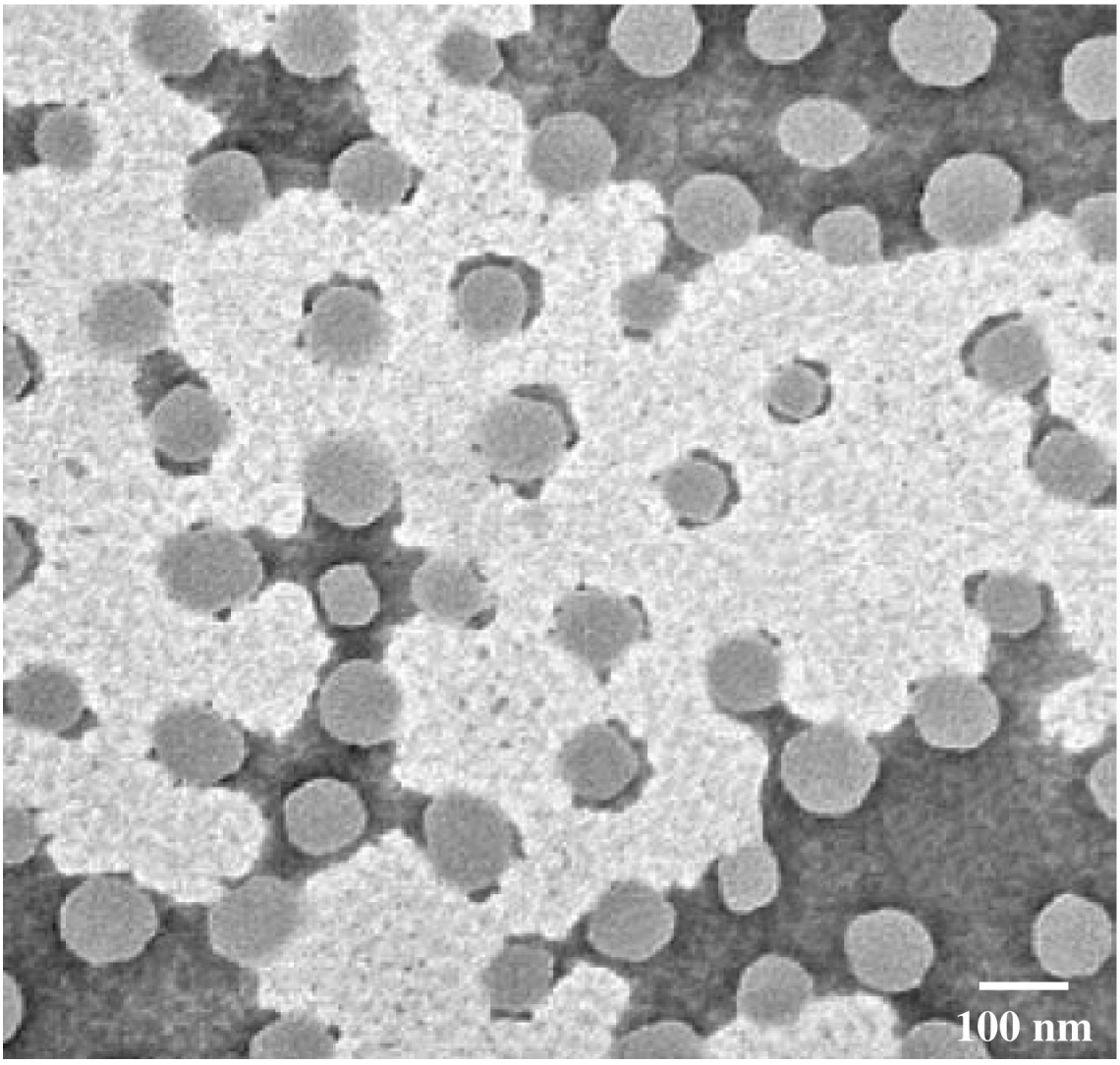

Fig. 3.
Transmission electron micrograph of NIPA-AAm-AH nanoparticles.

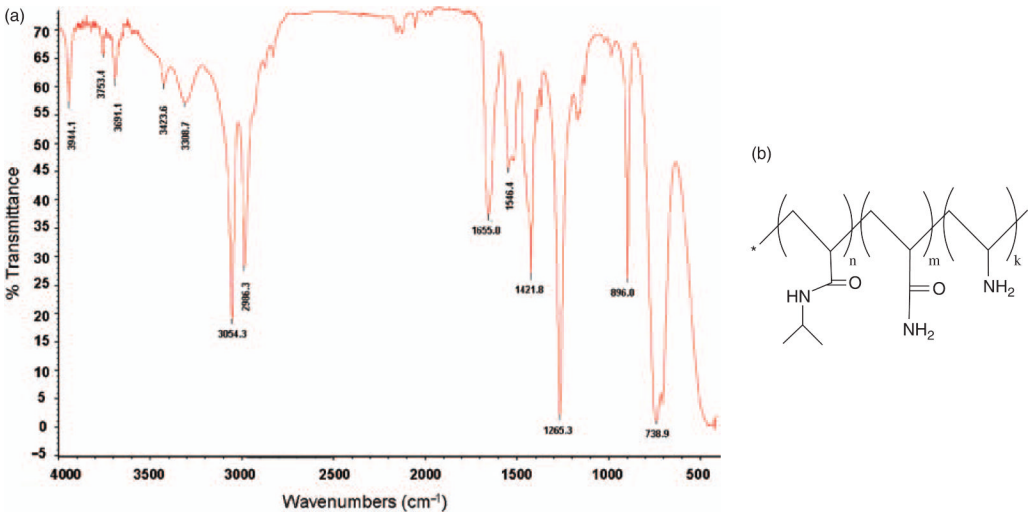

Fig. 4.

Chemical composition analysis of the nanoparticle. (a) FTIR spectrum of NIPA-AAm-AH nanoparticle at room temperature (25 °C). (b) Structure of NIPA-AAm-AH.

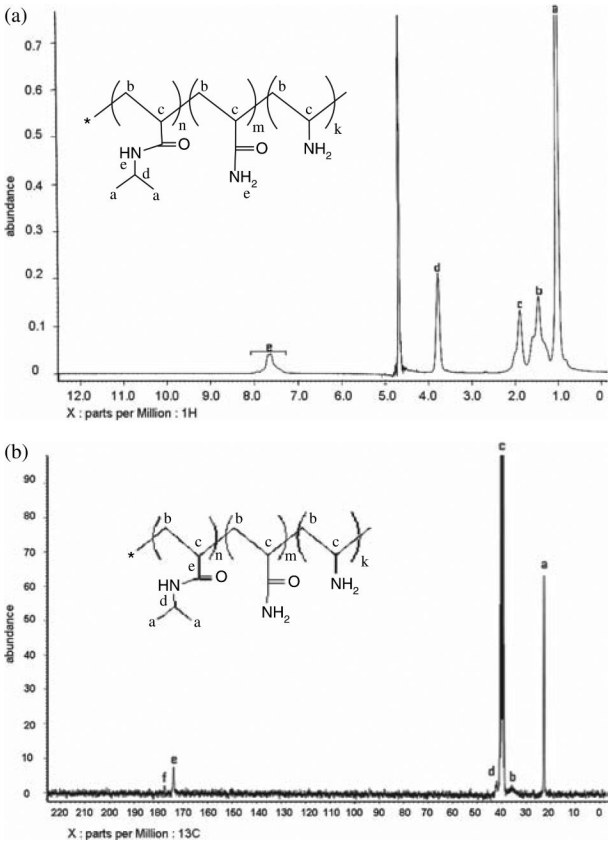

Fig. 5.
(a) ^{1}H NMR and (b) ^{13}C NMR spectra of NIPA-AAm-AH nanoparticles.

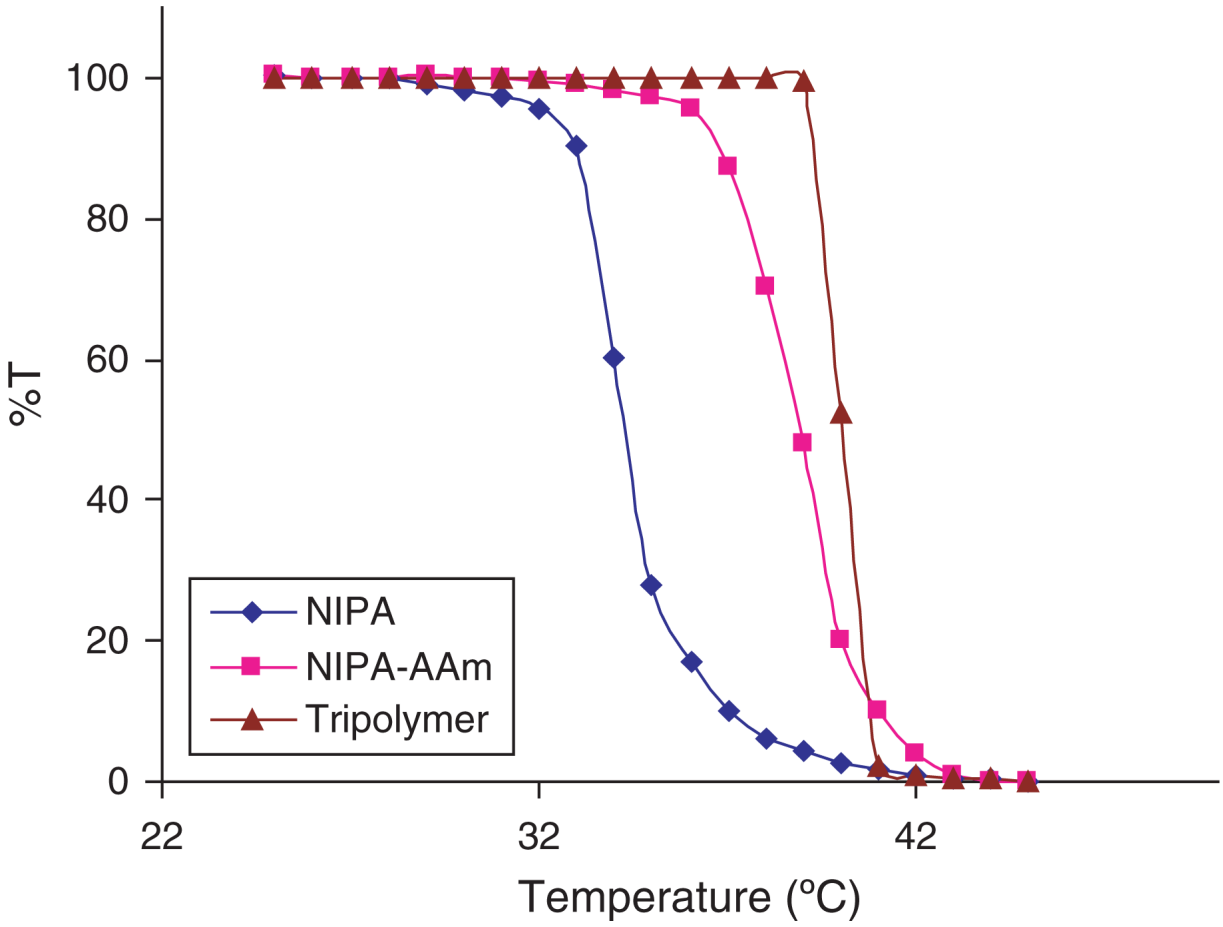

Fig. 6.
LCST of nanoparticles measured by using UV-Vis spectrophotometer.

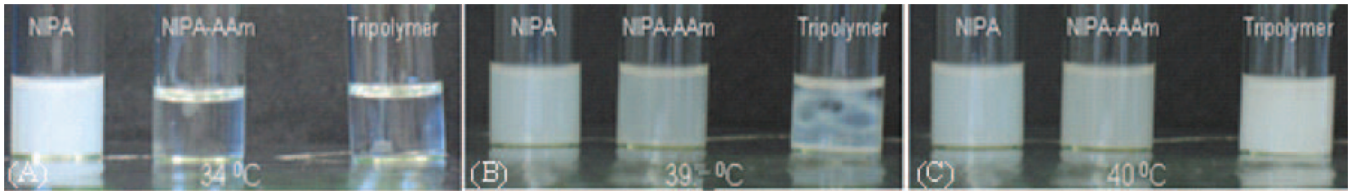

Fig. 7.

Photographs of NIPA, NIPA-AAm, and NIPA-AAm-AH nanoparticles at different temperatures. The nanoparticles were placed (A) at 34 °C, (B) at 39 °C, and (C) at 40 °C. A color change was observed when the phase transition occurred.

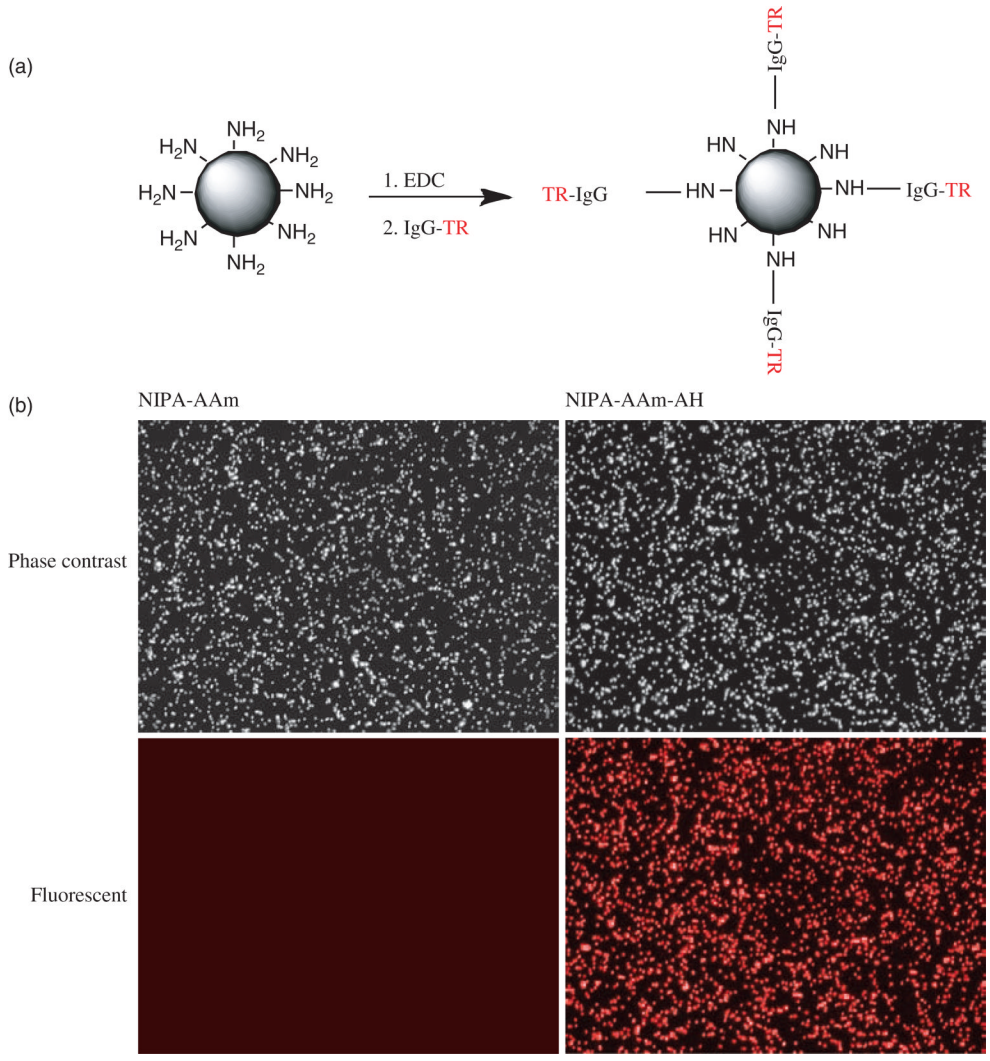

Fig. 8.

Conjugation of nanoparticles to IgG-TR (bovine anti-rabbit IgG-Texas Red). (a) Schematic diagram of the conjugation reaction of NIPA-AAm-AH nanoparticles with IgG-TR. (b) Fluorescent and phase contrast microscopy (cytoviva) images of NIPA-AAm and NIPA-AAm-AH nanoparticles reacted with fluorescent IgG.

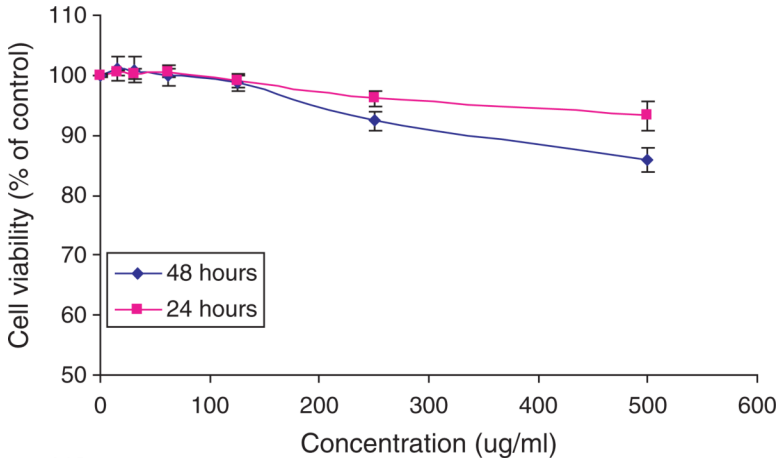

Fig. 9.

Cell viability of 3T3 fibroblast cells after 24 and 48 hours exposure to nanoparticles at various concentrations. The cell viability was assessed using MTS assays. Cells without exposure to nanoparticles served as controls.

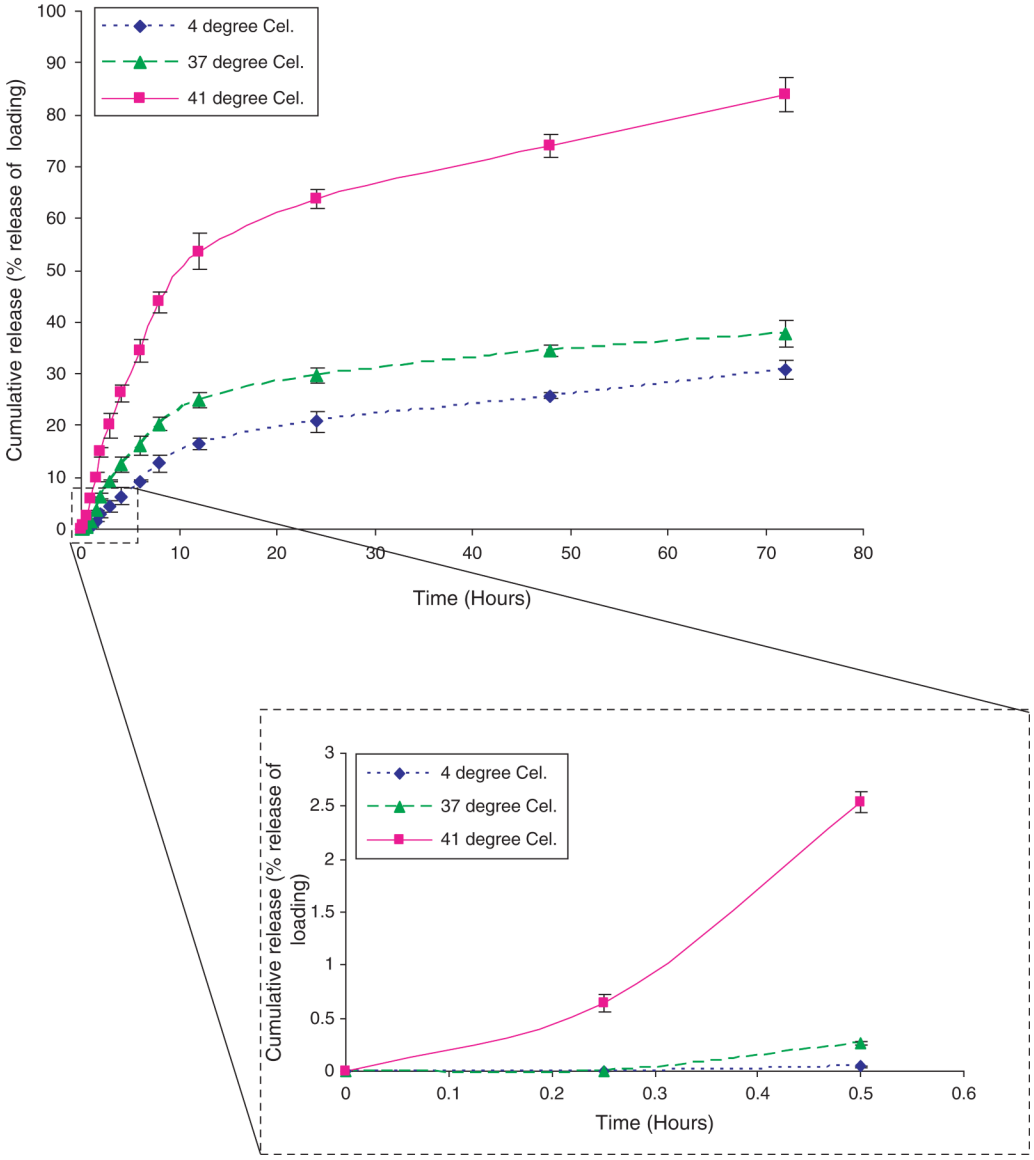

Fig. 10.

In vitro release profiles of DOX at 4 °C, 37 °C, and 41 °C over 72 hours. The insert is the cumulative percent release of DOX over 30 minutes.

Table I

Monomer ratio in the feed and in the NIPA-AAm-AH predicted by NMR and titration.

	In the feed	In the NIPA-AAm-AH
	$\times 10^{-3}$ mole (% mole)	% mole
NIPA	9.79 (58%)	61.9
AAm	2.00 (12%)	9.8
AH	5.05 (30%)	28.3